Structure and Dynamics of Membrane Proteins and Membrane Associated Proteins with Native Bicelles from Eukaryotic Tissues

*Sean T. Smrt‡, Adrian W. Draney‡, Indira Singaram and Justin L. Lorieau**

Department of Chemistry, University of Illinois at Chicago, 845 West Taylor Street, Chicago, Illinois 60607, United States

solution-state NMR, folch extraction, maldi-tof mass spectrometry,

ABSTRACT: *In vitro* studies of protein structure, function and dynamics typically preclude the complex range of molecular interactions found in living tissues. *In vivo* studies elucidate these complex relationships, yet they are typically incompatible with the extensive and controlled biophysical experiments available *in vitro*. We present an alternative approach by extracting membranes from eukaryotic tissues to produce native bicelles to capture the rich and complex molecular environment of *in vivo* studies while retaining the advantages of *in vitro* experiments. Native bicelles derived from chicken egg or mouse cerebrum tissues contain a rich composition of phosphatidylcholine (PC), phosphatidylethanolamine (PE), phosphatidylglycerol (PG), phosphatidylserine (PS), phosphatidylinositol (PI), phosphatidic acid (PA), lysolipids,

cholesterol, ceramides (CM) and sphingomyelin (SM). The bicelles also contain source-specific lipids such as triacylglycerides (TAGs) and sulfatides from egg and brain tissues, respectively. With the influenza hemagglutinin fusion peptide (HAfp) and the C-terminal Src Homology domain of Lymphocyte-specific protein-tyrosine kinase (lck-cSH2), we show that membrane proteins and membrane associated proteins reconstituted in native bicelles produce high-resolution NMR data and probe native protein-lipid interactions.

INTRODUCTION: Protein structure and membrane composition are interdependent in the function of membrane proteins. In cells, the complex composition of the membrane impacts its fluidity, charge distribution, curvature propensity and interaction with proteins. Specific lipids are known to influence the behavior of membrane proteins through molecular interactions and allosteric effects.[1–6] Despite the critical role of membrane composition on protein structure and function, the majority of structural and functional studies of membrane proteins are conducted *in vitro* with synthetic and homogeneous detergent or membrane formulations.

In vitro studies typically reconstitute membrane proteins in detergent micelles, vesicles comprised of synthetic lipid compositions, nanodiscs or lipid-detergent aggregates, known as bicelles.[7,8] Common detergents include dodecylphosphocholine (DPC), dihexanoylphosphatidyl-choline (DHPC) and octylglucosides, none of which are naturally abundant in living tissues. Detergent monomers can destabilize extramembraneous domains or partition into bilayered lipid regions.[9,10] Variations in hydrophobic thickness, gaussian curvature, lipid order parameters and the membrane bending modulus can affect the structure and dynamics of numerous membrane proteins. [11–16] These characteristics may be substantially different in micelles or small bicelles. Highly curved detergent micelles are known to distort protein structures and reduce the functional activity of membrane proteins.[17–19] In the case of diacylglycerol kinase (DAGK),

activity is maintained in micelles, but detergent-induced structural perturbations are seen when comparing the X-ray crystal structure with the oriented solid-state NMR structure.[20]

Nanodiscs and lipodiscs are alternative discoidal aggregates that avoid detergents altogether. Nanodiscs typically use amphipathic α-helical membrane scaffold proteins (MSPs) such as ApoA,[21] to entrap a bilayer region. Lipodics are formulated with polymers such as styrene maleic acids (SMA) .[22–24] Bicelles and nanodiscs can restore the functional activity of proteins characterized in micellar systems.[25,26] Nanodiscs have reasonable tumbling times for solution state NMR, but they require the purification of MSPs, which themselves present an additional protein into the system capable of producing unpredictable interactions with the protein of interest. Numerous solid-state NMR (SSNMR) protein structures circumvent curvature issues with extruded or freeze-thawed vesicles, yet these studies still typically use vesicles with non-native compositions of lipids.[27,28]

In vivo studies with "in cell" NMR give torsional and secondary structure information of biomolecules from chemical shifts.[29,30] In-cell NMR offers protein structural information directly in a cellular context, including the retention of native bilayer lipid composition asymmetry.[29,31] However, the high viscosity of the cytosol or cellular membrane environment leads to large tumbling times with a concomitant decrease in spectral resolution, and proteins may be localized in cellular inclusion bodies. Magic angle spinning (MAS) SSNMR can be applied to native tissues.[32] Such studies indicate an important correlation of lipid composition to dynamics and activity.

In this article, we report an *in vitro* approach using native bicelles prepared from the lipids of living tissues to study protein-lipid interactions. In contrast to traditional bicelle that contain only

small number of lipid types, native bicelles include the complex composition of lipids found in eukaryotic tissues. We show that membrane proteins and membrane associated proteins in native bicelles produce high-resolution NMR spectra amenable to detailed *in vitro* experiments, such as residual dipolar couplings (RDCs), needed for high-resolution structural and dynamic studies. When compared to traditional bicelles with DMPC, DPPC or POPC, we demonstrate that proteins reconstituted in native bicelles can be used to identify native protein-lipid interactions.

Low q-ratio bicelles, hereafter referred to simply as bicelles, are small discoidal lipid aggregates with a central region enriched in planar lipids and a rim capped by a detergent lipid. Bicelles are lipid-detergent aggregates that adopt either a mixed-micelle morphology, or a partially segregated bilayer and detergent rim aggregate with a discoidal shape.[33] Bicelles produce high-resolution NMR spectra of membrane proteins,[34] while offering a more oblate membrane aggregate that restores the function of membrane proteins previously impacted by micelles.[7,35] Initial studies have shown that lipids extracted from prokaryotes can be reconstituted into bicelles or nanodics.[36,37] Our native bicelles are reconstituted with purified lipids from eukaryotic tissues and show native protein-lipid interactions with eukaryotic systems.

While native bicelles are not bicomponent systems, we retain the nomenclature due to their similar behavior at low q-ratios and at high q-ratios, where they also form perforated lamellar 'aligned bicelles' that orient in a magnetic field (Figure S1). These bicelles are 'native' because they include the broad distribution of native lipids from living tissues, as compared to synthetic bicelles with only a few lipid components. We show that a comparison of protein spectra in non-native and native bicelles can help identify the presence of protein-lipid interactions. We use this information to guide titration experiments with specific lipids, such as PIP3, in non-native bicelles to identify which lipids in the complex mixture of native bicelles are influencing a

protein's structure. Native bicelles share many of the advantages of *in vivo* studies. In comparison to detergent micelles, they present lipid aggregates, like traditional bicelles, closer to a native membrane morphology. They also incorporate a complex mixture of cellular lipids that may be useful in revealing native biochemical interactions of membrane proteins and membrane associated proteins.

MATERIALS AND METHODS:

Extraction of Native Lipids. Lipids were extracted from chicken egg yolks and mouse cerebrum by homogenizing with a mixture of 2:1 chloroform (Sigma-Aldrich) to methanol (Sigma-Aldrich), washing the solution twice with water in a 7:2 organic solvent to water ratio before decanting the organic layer. The extract was washed once more with water in a separatory funnel. The organic phase was then lyophilized and reconstituted in a 2:1 chloroform to methanol mixture before aliquoting and lyophilization. Prior to use, aliquots were resuspended in water and passed through a 0.22 μm filter. After the addition of DHPC solution to the lipid extract and vortexing, each sample was put through five freeze/thaw cycles by submersion in liquid nitrogen.

The composition of the egg bicelle samples (E-bicelles) before and after the final filtration step was measured using ^{13}C-HSQC spectra of samples dissolved in d-chloroform (Sigma-Aldrich). Statistics on the variability of composition were conducted for 5 extractions of different egg samples. From measurements of the extracts in d-chloroform, it was found that the final filtration step largely removed triacylglycerides (TAGs). The average final composition of the native E-bicelles measured for 5 samples is listed in Table S1 and the final composition of MB-bicelles is

listed in Table S2. Additionally, we include in the SI a ^{31}P NMR spectrum (Figure S2) with the assignments of phospholipids in total porcine brain extract (Avanti) from a commercial source.

NMR Sample Preparation. HAfp samples with either ^{2}H ,^{13}C,^{15}N- or ^{15}N-isotope labeling were expressed and purified as previously described.[38] NMR samples contained 350-600 μM HAfp in 25 mM Tris (Fisher) pH 7.3 buffer with 10% deuterium oxide ($^{2}H_2O$, Sigma-Aldrich). Samples were prepared in 125 mM DHPC (Anatrace) titrated to 0-60 mM DMPC (Anatrace), or 42 mM native egg lipid with 142 mM DHPC (Anatrace) (q=0.34 E-bicelles). The q-ratio is the ratio in concentration of the planar lipid to the detergent lipid, which in this case was DHPC. The native E-bicelle q-ratio was calculated with the lipid concentrations determined from peak integrals in ^{31}P and ^{13}C-HSQC spectra. The added DHPC concentration was known, and the DHPC peaks were used as an internal standard.

Aligned samples for RDC measurement in the HAfp E-bicelle system were prepared with the addition of 18 mg/ml pinacyanol acetate, as described previously,[39] to 400 μM ^{15}N-HAfp in a 25 mM Tris pH 7.3 buffer with 10% $^{2}H_2O$, 24 mM native egg lipid and 89 mM DHPC (q=0.27). Alignment was verified by measurement of the residual quadrupolar coupling of $^{2}H_2O$, which was 40.4 Hz.

Lck-cSH2 samples with ^{2}H ,^{13}C,^{15}N- and ^{15}N-isotope labeling were expressed and purified as previously described.[40] NMR samples were prepared with 300-380 μM Lck-cSH2 in 20 mM Tris pH 7.0 buffer with 100 mM NaCl, 1 mM DTT and 10% $^{2}H_2O$. We studied the Lck-cSH2 in two systems: in synthetic DPPC bicelles and in native bicelles from mouse cerebrum tissues (MB-bicelles). The DPPC bicelle samples contained 50 mM DPPC (Affymetrix) and 100 mM DHPC (q=0.50). These were prepared with 10 minutes of 40 °C incubation to assist in the bicelle

formation and equilibration. The titration of DPPC bicelle samples with phosphatidylinositol-3,4,5-triphosphate (PIP3) was performed with 12 µl aliquot additions of 5 mM phosphatidylinositol-3,4,5-triphosphate C-16 (PIP3-DPPC, Cayman Chemical) up to a final sample concentration of 588 µM. The Lck-cSH2 samples in the presence of MB-bicelle were prepared identically with the inclusion of q=0.29 MB-bicelles formulated with 15.2 mM mouse cerebrum lipid and 51.4 mM DHPC.

A q-ratio titration was performed by adding aliquots of 200 mM DMPC solution to the previously described ^{15}N-HAfp23 sample in 125 mM DHPC. The 200 mM DMPC titrant solution was a turbid suspension. To accurately quantify the amount of DMPC added, as well as the corresponding q-ratio, the final concentrations were calculated from the ^{1}H 1D integrals of the terminal methyl peaks of DMPC and DHPC.

A high-q aligned E-bicelle sample to test the alignment of the bicelles themselves (Figure S1) was prepared with 114 mM native egg lipids and 25 mM DHPC in 25 mM Tris pH 7.4 buffer and 10% $^{2}H_2O$. The sample was then submitted to 5 freeze thaw cycles.

Finally, a native bicelle sample was prepared in 105 mM DHPC with 30 mg/mL porcine brain lipids (PB-bicelle, Figure S2), corresponding to 38 mM native lipids, in 25 mM Tris at pH 7.4 with 10% $^{2}H_2O$.

NMR Experiments. NMR experiments were collected using a 500-MHz Bruker Avance III HD spectrometer equipped with a ^{1}H/^{13}C/^{15}N/^{31}P QXI room temperature probe with triple-axis gradients. Gradients were calibrated using the residual $^{1}H^{2}HO$ signal in a 99.9% $^{2}H_2O$ sample at 25.0 °C with a published[41] translational diffusion constant of $1.902 \pm 0.002 \times 10^{-9}$ m^2 s^{-1}. The z, y, and x gradient strengths were found to be 58.7, 44.6, and 44.0 G/cm, respectively, at their

maximum currents. All spectra were collected at 32.0 °C, which was calibrated by measuring the chemical shift difference of the $^{1}H_3C$ and ^{1}HO resonances in a methanol standard with an estimated precision of 0.1 °C. Native lipid concentrations were quantified by ^{1}H 1D, ^{13}C-HSQC and ^{31}P 1D NMR spectra using the $^{1}H_2O$ resonance, the DHPC ^{1}H-^{13}C resonances, the DHPC ^{31}P resonance and the ^{31}P resonance of trimethyl phosphate, as internal standards.

The peak assignment for the ^{15}N-HSQC spectra of Lck-cSH2 was achieved using chemical shift values previously assigned[42] and verified with the use of multiple triple resonance NMR experiments collected on the ^{2}H ,^{13}C,^{15}N-labeled samples. HNCA, HNCACB, HNCO and (H)CCH-TOCSY spectra were collected at 500 MHz, all with Rance-Kay detection.[43]

Chemical shift perturbations (CSPs) were calculated from root-mean square deviations (RMSDs) in the chemical shifts, using a ^{15}N scaling factor α=0.2 for glycine residues and α=0.14 for all other residues.[44,45]

$$RMSD = \sqrt{\frac{1}{2}\left(\delta_H^2 + \left(\alpha \cdot \delta_N^2\right)\right)} \quad (1)$$

The ^{1}H-^{15}N J-couplings and RDCs were measured at 500 MHz using an IPAP-WATERGATE sequence.[46] RDCs were extracted from the data using NMRPipe and Sparky.[47,48] The 2KXA structure of HAfp[49] was used as the reference model in the singular value decomposition (SVD) analysis of the measured PNA RDCs in native lipids.[50] The Q-factor of the fit was subsequently calculated using NMRPipe.[47,51]

Composition of Native lipids. Native lipid compositions were determined with the peak integrals from ^{1}H and ^{31}P 1D NMR spectra and a ^{13}C-HSQC 2D spectrum. The concentrations of $^{1}H_2O$ and DHPC were known, and the resonances from these molecules were used as internal

standards for quantitating lipid concentrations. Due to differences in coherence transfer efficiencies for AX, AX_2 and AX_3 spin systems,[52] ^{13}C-HSQC peak integrals for each spin system type were corrected by observing their relative intensities from pure POPC (Anatrace), POPE (Anatrace), or cholesterol (Sigma-Aldrich) samples collected in d-chloroform. These pure samples were additionally used to confirm chemical shift assignments.

The native lipids were identified and quantified from resonances in the head group region.[53,54] Although the exact acyl chain distribution cannot be distinguished by NMR, the types of unsaturated lipids can be quantified in terms of oleic, linoleic, and linolenic types, based on the unique ^{1}H-^{13}C correlations of the vicinal hydrogens.[55] Five separate extractions of egg lipids were performed and the native lipid components of E-bicelles were quantified (Table S1) before and after filtration through a 0.22 μm polyvinyldene difluoride (PVDF) filter. The error in quantifying the egg lipids was determined by calculating the standard deviation of each of the lipid components across the five different egg extractions. A minimum error was set at 0.1 mol% for all components.

Mass Spectrometry. Mass spectrometry was conducted on an Applied Biosystems 4700 Proteomics Analyzer MALDI-TOF. 200 iteration scans were performed in positive and negative reflectance modes with a 200 Hz laser. Samples were deposited on an A&B etched-well, matrix-assisted laser desorption ionization (MALDI) plate. A 0.5 μL spot of saturated Universal MALDI Matrix (Fluka) with 50% (v/v) acetonitrile and 0.1% trifluoroacetic acid (TFA, v/v) was deposited before and after the addition of the native lipid sample. Mass peaks and their assignments are reported in Tables S3 and S4 for egg lipid and mouse brain extracts, respectively, with assigned spectra shown in Figures S3-S5. Numerous poly-acyl lipids have degenerate masses, which are associated to multiple hydrophobic tail configurations.

Consequently, the tail lengths have been reported as the summation of carbons and the summation of unsaturated bonds, as previously described.[56,57] Ceramides are reported as mono- and di-hydroxyl with an 'm' and 'd' prefix, respectively. In some cases, an observed mass can be attributed to multiple lipid types. Alternative possibilities are listed in the assignment tables. Reported head group types were validated with ^{31}P and ^{13}C NMR measurements and have been previously identified in egg and brain tissues.[58–62] A large portion of triacylglyceride molecules are present as deacylated diacylglyceride fragments with associated wax ester fragments due to the low pH sample preparation.[63]

RESULTS AND DISCUSSION: Native bicelles are prepared with lipids and membrane components from lysed eukaryotic cells, and they are solubilized into small discoidal lipid-detergent aggregates with a detergent capping lipid, DHPC. The size of the aggregates is easily tuned by changing the molar ratio, q-ratio, of native lipids to detergent lipids. At high q ratios, these native bicelles display an alignable bicelle phase similar to previously measured bicelles (Figure S1) that have been used to measure RDCs in soluble proteins.[64] Native lipids are extracted using a modified Folch method[65] that largely removes aqueous components and cellular proteins. We chose to use a Folch method to remove endogenous proteins and avoid additional protein-protein interactions. We demonstrated this approach using lipids from chicken (*Gus gallus*) egg yolk (E-bicelles) and from female BALB/c mouse cerebrum (*Mus musculus*, MB-bicelles).

The ^{31}P spectrum (Figure 1) and ^{13}C HSQC NMR spectra (Figure S6-S7, Table S5) in combination with positive and negative reflectance MALDI-TOF mass spectra (Figures 2, S3-S5, Tables 1-2, S3-S4) show a rich composition of PC, PI, PG, PE, PS, PA, SM, cardiolipin (CL), CM lipids with mono- (lyso), di- and tri-acyl variants, as well as numerous tissue specific

lipids and some unidentified lipids (U). The ^{1}H 1D NMR spectra (Figure S8) and Bradford assays confirm the absence of endogenous proteins.

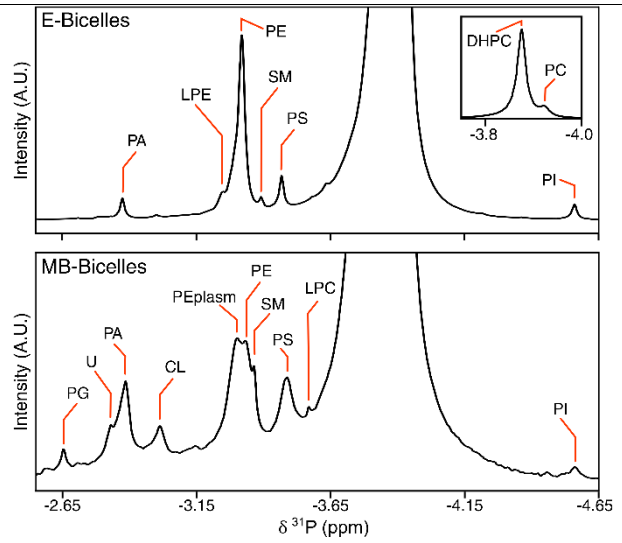

Figure 1. ^{31}P 1D NMR spectra of (top) q=0.34 native E-bicelles and (bottom) q=0.37 native MB-bicelles in 25mM Tris at pH 7.4 with 10% $^{2}H_2O$. The lipid headgroups were identified from reference chemical shifts[53,54] and are listed in Table S5. All ^{31}P chemical shifts are reported relative to trimethyl phosphate. Spectra were collected at 202.5 MHz ^{31}P frequency (500 MHz ^{1}H NMR field) at 25.0°C with ^{1}H decoupling. The inset image provides a zoomed-out view to emphasize the distinct DHPC and PC peaks.

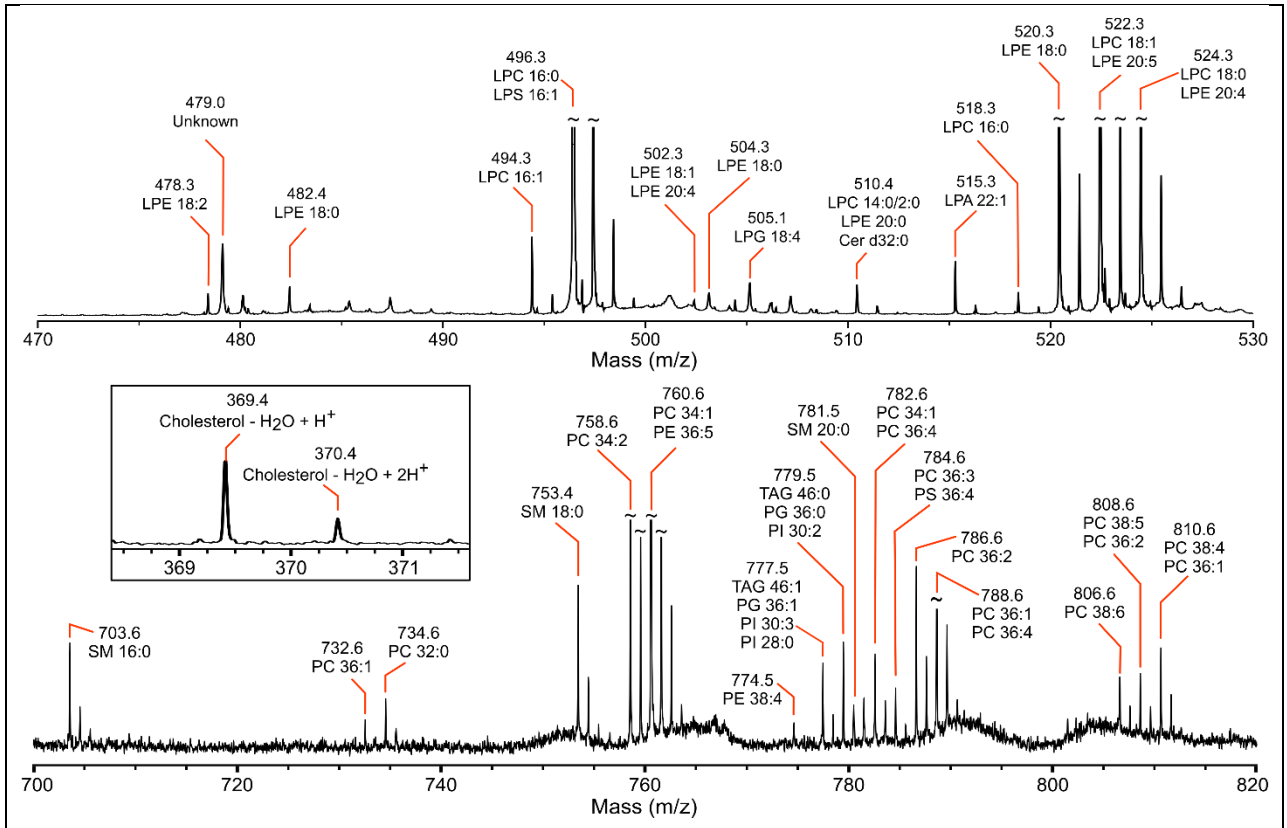

Figure 2. Positive reflectance MALDI-TOF mass spectra of egg yolk lipid extract. Assignments are presented with headgroup acronyms and acyl chains represented as a summation of carbons to saturations to describe all degenerate masses. Full spectra for both egg yolk and mouse cerebrum are presented in Figures S3-S5.

Native E-bicelles are composed of PC (64 ± 3 mol%), PE (16 ± 2%), TAG (8 ± 4%), cholesterol (8 ± 2%), LPC (1.3 ± 0.3%), LPE (1.3 ± 0.6%), SM (1.1 ± 0.4%), and PS (0.9% ± 0.3%) with a high degree of unsaturated lipids (ca. 51% with at least 1 unsaturation), which are consistent with previously measurements.[66] The lipid extracts further contain trace amounts of vitamins, flavonoids, carotenoids, and amino-acids present in living membranes. These components have all been previously identified in egg yolk, but they have not been confirmed to

incorporate into bicelle samples.[66,67] Native MB-bicelles are composed of cholesterol (45 ± 3%), PC (29 ± 2%), PE plasmalogens (9 ± 4%), PE (5 ± 2%), PA (4 ± 1%), PS (3 ± 1%), SM (1.3 ± 0.5%), PG (0.7 ± 0.3%), CL (0.7 ± 0.3%), PI (0.6 ± 0.2%), LPC (0.2 ± 0.1%) and other lipids (1.1 ± 0.4), which are consistent with previous measurements.[62] Mouse brain lipids also have a high (*ca*. 41%) degree of unsaturation. MALDI-TOF spectra of the mouse brain lipids showed the presence of other lipids not readily identified by NMR, including sulfatides, ceramides, phosphatidylinositol phosphate (PIP) and phosphatidylinositol 4,5-bisphosphate (PIP2). PIP3 was not detectable by MALDI-TOF spectrometry,[68] but it is a ubiquitous signaling lipid present in mouse brain tissue.[69,70]

Table 1. An abbreviated list of assignments for the m/z values of the egg lipid components detected by positive reflectance ion MALDI-TOF mass spectrometry [a,b]

Peak Position (m/z)	**Assignment of molecular Mass**
369.4	Cholesterol - H_2O + H^+
482.4	LPE 18:0 + H^+
496.3	LPC 16:0 + H^+; LPS 16:1 + H^+
524.3	LPC 18:0 + H^+; LPE 20:4 + Na^+
526.3	LPE 22:6 + H^+
544.4	LPS 18:2 + Na^+
546.4	LPC 18:0 + Na^+
552.7	Crypoxanthin
560.3	PC 18:0 + Na^+; Cer d34:1 + Na^+
568.3	Zeaxanthin
568.4	LPC 22:6 + H^+; PS 20:0 + H^+

570.4	PS 22:6 + H^+; LPC 22:5 + H^+
577.5	TAG 52:2 - oleate + Na^+; TAG 52:1 - stearate + Na^+
608.7	PE 26:0 + H^+; Cer m40:0 + H^+
703.6	SM 16:0 + H^+
732.6	PC 32:1 + H^+
753.4	SM 18:0 + Na^+
760.6	PC 34:1 + H^+
777.5	TAG 46:1 + H^+; PG 36:1 + H^+; PI 30:3 + H^+
779.5	TAG 46:0 + H^+; PG 36:0 + H^+; PI 30:2 + H^+
781.5	SM 20:0 + Na^+
788.6	PC 36:1 + H^+
812.7	PC 36:0 + Na^+; PE 40:7 + Na^+
834.7	PS 38:4 + H^+
964.9	PE 52.4 + H^+
975 – 1125	Numerous Triacylglycerides

a. Assignments are described with adducts and acyl chains presented as a summation of carbons to saturations to describe all degenerate masses.
b. A complete table with references to assignments is presented in Table S3.

Table 2. An abbreviated list of assignments for the m/z values of the mouse cerebral lipid components detected by positive and negative reflectance ion MALDI-TOF mass spectrometry [a,b]

Peak Position (m/z)	**Assignment of molecular Mass**
369.4	Cholesterol - H_2O + H^+

468.4	LPC 14:0 + H^+
496.3	LPC 16:0 + H^+; LPS 16:1 + H^+
504.3	Cer d30:1 + Na^+ ;LPE 18:0 + Na^+
524.3	LPC 18:0 + H^+ ;LPE 20:4 + Na^+ ;Cer m24:0 + H^+
539.3	LPG 20:1 + H^+
550.5	LPC 20:1 + H^+ ;Cer m36:1 + H^+
557.3	LPG 22:6 + H^+
593.4	LPA 28:0 + H^+
711.4	PE 34:4 + H^+
731.6	SM 18:0 + H^+
748.5	PE 38:6a + H^+
750.4	PE 38:4p – H^+
760.5	PC 34:1 + H^+
762.5	PC 34:0 + H^+
763.3	PG 36:7 – H^+
774.5	PE 38:4a + Na^+
788.6	PS 36:1 – H^+ ;PC 36:1 + H^+
790.5	PE 40:6a – H^+ ;PS 36:0 – H^+
795.4	PG 38:5 – H^+ ;PA 44:1 – H^+
806.5	ST 18:0 – H^+ ;PS 38:6 – H^+
809.5	PI 32:1 + H^+ ;PA 44:4 + H^+
810.6	PS 38:4 – H^+
822.5	ST 18:0 + OH – H^+
832.6	PE 42:0 + H^+; PS 40:8 + H^+
834.5	PS 40:6 – H^+; ST 20:0 – H^+; PC 40:6 + H^+
857.4	PI 36:4 – H^+
862.6	ST 22:0 – H^+
885.5	PI 38:4 – H^+
890.6	ST 24:0 – H^+
904.6	ST 24:1 + OH – H^+
965.6	PIP 38:4
1045.5	PIP2 38:4

a. Assignments are described with adducts and acyl chains presented as a

summation of carbons to saturations to describe all degenerate masses.
b. A complete table with references to assignments is presented in Table S4.

We used the full-length influenza hemagglutinin fusion peptide domain (HAfp) as a control system for testing native bicelles. HAfp is functional in eukaryotic lysosomal membranes,[71] and it is an amphipathic membrane protein that folds in the presence of lipid membranes.[72] HAfp has an amphipathic helical-hairpin structure with a hydrophobic base that binds to the membrane surface. We tested HAfp in E-bicelles since largescale vaccine production for the influenza virus uses fertilized hen eggs to culture viral replication.[73] HAfp is fusiogenic in vesicles composed of egg yolk native lipids (Figure S9). HAfp in native E-bicelles with q=0.34 produces high-resolution ^{15}N HSQC 2D spectra (Figure 3A) with a spectral resolution comparable to the protein in DMPC bicelles. The native E-bicelle chemical shifts are nearly indistinguishable from DMPC bicelles; the mean CSPs between DHPC micelles and E-bicelles are *ca*. 5.2x larger than those measured between DMPC bicelles and E-bicelles (Figure 3B). These CSPs are not significant enough to indicate a large structural rearrangement between micelle and bicelle samples. However, they're consistent with modest structural distortions in the helices themselves. Differences in CSPs from the bending of helices induced by micelle curvature strain was observed previously in other membrane protein systems.[18,35,74,75] The magnitude of these CSPs are also consistent with previous measurements on different micelle environments, which have different aggregation numbers, micelle sizes and surface curvatures. [76–78]

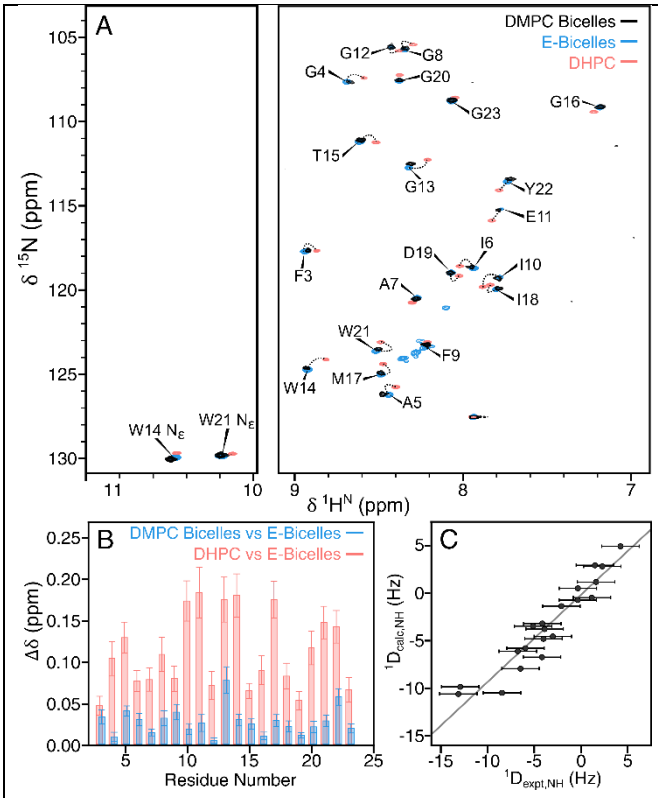

Figure 3. (A) ^{15}N-HSQC spectrum for 350-600 μM HAfp in 25 mM Tris pH 7.3 with 10% $^{2}H_2O$ solubilized in DHPC micelles, q=0.46 DMPC bicelles and q=0.34 native E-bicelles. (B) HAfp CSPs between E-bicelles and DHPC micelles or DMPC bicelles. (C) Singular value decomposition fit of the HAfp ^{1}H-^{15}N RDCs from a q=0.27 native E-bicelle sample in 18 mg/ml PNA liquid crystal.[39] The structure was fit to the published HAfp structure in DPC micelles (PDB: 2KXA[49]). This structure also accurately fits to HAfp in synthetic DMPC bicelles.[79] The fit D_a and Q-factor were -7.8 Hz and 16.0%, respectively.[51]

There is still some debate on the exact morphology of bicelles and the extent of lipid segregation between the bilayer lipid and the capping lipid, with smaller bicelles believed to have more of a mixed-micelle composition. Larger bicelles, with a $q \geq 0.5$, are nonetheless believed to form aggregates that are more discoidal in structure with a highly segregated

bilayered region.[9,80,81] Therefore, we chose to use native bicelles of comparable size to q = 0.5 DMPC and POPC bicelles as calculated from rotational tumbling times and translational diffusion rates derived from ^{31}P relaxation and diffusion ordered spectroscopy (DOSY). In the case of HAfp, a titration of DMPC into DHPC micelles yields a plateau in CSPs at a q-ratio near *ca*. 0.40 (Figure S10). Additionally, intermolecular NOEs between DMPC and HAfp, but not DHPC and HAfp, have previously been measured.[82] These measurements suggest that HAfp partitions into a DMPC-rich central region of the DMPC bicelles.

NMR relaxation and DOSY experiments show that these E-bicelles are small, isotropically tumbling bicelles with a size between DMPC and POPC bicelles with a comparable q-ratio. Backbone ^{15}N relaxation rates for HAfp in q=0.34 native E-bicelles (Figure S11) give an effective rotational tumbling time of 19.7 ± 0.2 ns. This tumbling time is similar to the 21.0 ± 0.3 ns value from HAfp in q=0.52 DMPC bicelles.[79,82] E-bicelles are expected to form larger aggregates than DMPC bicelles for a given q-ratio because egg lipids are composed of larger lipids, like POPC lipid (Mw: 761 g/mol), as opposed to DMPC (Mw: 678 g/mol). However, the ^{15}N relaxation data alone is subject to differences in protein order parameter between samples, and the quantitative deconvolution of the effective rotational tumbling time from the bicelle size can be a challenge. [82]For these reasons, we conducted further relaxation and translational diffusion (DOSY) experiments.

DOSY NMR and ^{31}P relaxation NMR measurements (Figure S12) further confirm that native E-bicelles are phospholipid aggregates with a size between DMPC and POPC bicelles.[83] To account for the 8-11 mM free concentration of detergent not bound to bicelles, the sizes of native E-bicelles were measured as a function of effective q_e-ratios. For a q_e-ratio of 0.30, the native E-bicelles are *ca*. 82% larger than DMPC bicelles and *ca*. 30% smaller than POPC bicelles. The

smaller size of E-bicelles in comparison with POPC bicelles is consistent with the lighter PE lipids (POPE Mw: 718 g/mol) and cholesterol present in E-bicelles. While this does not guarantee that DHPC segregates exclusively to the rim, it suggests that the native bicelle morphology is likely similar to DMPC or POPC bicelles at q-ratios as low as q=0.34. This is further substantiated by the HAfp CSP data (Figure 3B) that show that native bicelles are closer to DMPC bicelles than both DHPC and DPC micelles (Figure S13).

While the HAfp structure is not impacted by membrane composition, we tested the impact of specific protein-lipid interactions with the C-terminal Src Homology domain of Lymphocyte-specific protein-tyrosine kinase (Lck-cSH2). Lck-cSH2 is a 13 kDa domain that binds to phosphorylated-tyrosine.[84] We chose Lck-cSH2 as a reference system since it is a membrane-associated domain with known protein-lipid interactions, including PIP, PIP2 and PIP3.[40]

In the presence of DHPC micelles, Lck-cSH2 shows CSPs consistent with minor structural changes or non-specific interactions (Figure S14A) due to the DHPC micelle environment or the free DHPC monomer. These CSPs are reduced by the addition of DPPC to formulate q=0.5 bicelles (Figure S14B). Similar to HAfp, this difference is not unexpected and could be the result of the artificial stress produced by highly curved micelles. However, in the presence of MB-bicelles, a separate set of perturbations occurring at different residues is measured (Figure 4A). These site-specific CSPs measured in the presence of MB-bicelles are primarily localized to a known positive binding pocket (Figure 4B), and they are consistent with previously reported PIP3 dependent shifts.[85]

We compared the MB-bicelle CSPs to CSPs observed in DPPC bicelles with PIP3-DPPC (Figures 4A, S14-S15). The PIP3-dependent shifts observed in native bicelles include R134, R154, E155, S156, E157, G161, F163, L165 and R184. Other PIP3-dependent shifts (N131,

S164, V178 and H180) do not appear in MB-bicelles and may be additionally impacted by the non-native DPPC bicelle system. It is also possible that interactions with other anionic lipids present in MB-bicelles, such as PIP, PIP2, PG or PA, at or near the PIP3 binding pocket produces a slightly modified CSP profile. The differences (residues I183, S197 and H208) may point to other protein-lipid interactions in the native function of the Lck-cSH2.

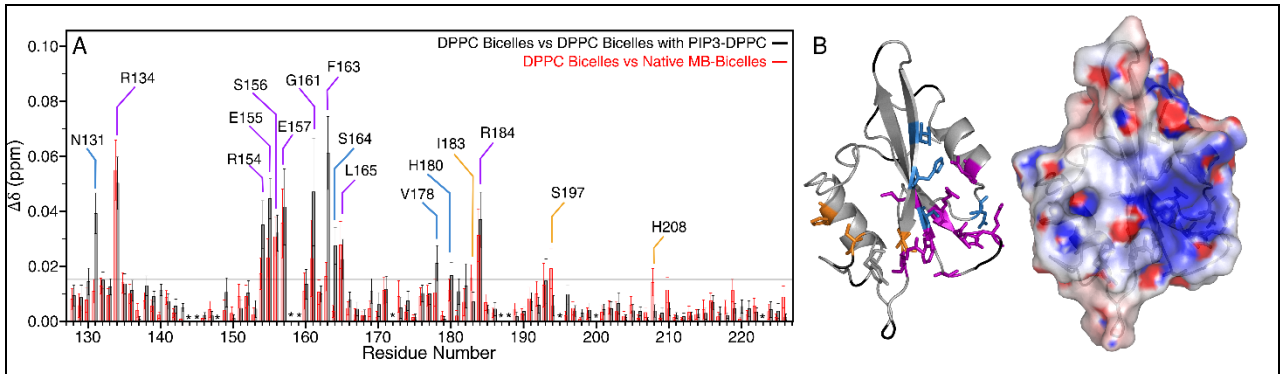

Figure 4. (A) CSPs for 380 μM ^{15}N-labeled Lck-SH2 in 20 mM Tris, 100 mM NaCl and 1mM DTT at pH 7.04 in the presence of 150 mM (total lipid) q=0.5 DPPC bicelles titrated with 312 μM PIP3-DPPC (black) or 67 mM q=0.29 MB-bicelle (red). A threshold of 0.015 was chosen to indicate significant CSPs based on those measured in the presence of bicelles alone (Figure S14B). Residues absent from the HSQC spectra were excluded from the CSP analysis and are indicted by an (*) in the bar chart or presented in black on the molecule. These residues are primarily located in unstructured loop regions, as well as proline residues, which lack the backbone amides necessary for ^{15}N-HSQC measurement. (B) Significant CSPs were mapped onto the structure (PDB: 1BHH, left structure) as affected by PIP3-DPPC (blue), MB-bicelles (orange) or by both (purple). An Adaptive Poisson-Boltzmann Solver (APBS) electrostatic surface generated at pH 7 (right structure) shows positive residues colored in blue and negative residues colored in red.

CSPs in native bicelles are observed, even though some of the membrane components are in low abundance. Lipids and membrane components with low concentrations are likely not present in every native bicelle aggregate in the sample. However, membrane proteins with high affinities to specific lipids may enrich the local concentration of these lipids within their bicelles. The Lck-cSH2 domain, for instance, has a high affinity for negatively charged lipids.[40] In this circumstance, low abundance lipids would be recruited to bicelles with Lck-cSH2 through high affinity protein-lipid interactions. Additionally, the magnitude of CSPs is scaled by the population of proteins bound to the membrane.[45] A protein such as Lck-cSH2, which has a bound population of 5 ± 4% in MB-bicelles (Figure S16), is expected to have less substantial CSPs compared to a membrane protein such as HAfp which has a bound population of 81 ± 11% in DMPC bicelles.[38]

Though native bicelles are not a perfect mimic for biological membranes, the inclusion of native lipids in the bicellar environment is a step closer to emulating a biological membrane *in vitro*. The fusion activity of HAfp is higher in the presence of cholesterol,[86,87] yet cholesterol, among other native lipids, do not impact the helical-hairpin HAfp structure. Consequently, our results substantiate a cholesterol-dependent fusion enhancement through bulk membrane properties, rather than a modulation of the protein's structure. In the Lck-cSH2 system, numerous CSPs are observed in the presence of the complex mixture of the native MB-bicelles. These include interactions with negatively charged lipids, like PIPs.

In addition to offering structural and dynamic information on membrane proteins in a native membrane environment, native bicelles can serve as a useful starting point in directed titration experiments for specific lipids in synthetic DMPC or DPPC bicelles. Native bicelles also display an alignable bicelle phase at high q ratios that exemplifies the familiar bicelle utility these

systems can provide and which may offer orthogonal RDC datasets of soluble proteins. Variation in the lipid composition of different tissue types is expected and has been well characterized. Our experience shows that this technique is simple enough to act as a routine starting point for characterizing membrane proteins. While membranes undergo constant remodeling, supplemental techniques including fluorescent microscopy may be useful in identifying spatiotemporal restrictions once general protein-lipid interactions are established. The choice of tissue type can be specific to the native environment of a protein-of-interest, with some lipid extracts already commercially available and amenable to immediate solubilization into bicelles (Figure S2). Other possibilities include the generation of organelle or leaflet-specific membranes that are routine to purify,[88–91] or the incorporation of native lipids in nanodics. Native bicelles provide a platform for studying membrane protein-lipid interactions central to their function in an environment suitable for biophysical experiments while retaining the native-like composition found in eukaryotic cells.

ASSOCIATED CONTENT

Supporting Information. The Supporting Information is available free of charge on the ACS Publications website at DOI: xxx-xx

Additional methods pertaining to relaxation and DOSY NMR measurements, Bradford assay and lipid-mixing fusion assay. Additional figures and tables containing ^{1}H 1D and ^{1}H-^{13}C HSQC spectra of native bicelles, MALDI-TOF mass spectra with tabulated assignments, lipid-mixing fusion assay, backbone relaxation of HAfp, DOSY translational diffusion of bicelles, ^{1}H-^{15}N HSQC spectra of Lck-SH2 with measured CSPs, tabulated native bicelle composition.

The following files are available free of charge.

Supporting_Figures.PDF

AUTHOR INFORMATION

Corresponding Author

*justin@lorieau.com

Author Contributions

‡S.T.S. and A.W.D. contributed equally.

Funding Sources

This work was supported by the NSF (#1651598)

Notes

The authors declare no competing financial interests.

ACKNOWLEDGMENT

A special thank you to Wonhwa Cho for providing lck-cSH2 protein, Stephanie Cologna for providing mouse cerebral tissues and helpful discussions and Bhagya Mendis for assistance in preparing samples and figures.

ABBREVIATIONS

PC, phosphatidylcholine; PE, phosphatidylethanolamine; PG, phosphatidylglycerol; PS, phosphatidylserine; PI, phosphatidylinositol; PA, phosphatidic acid; CM, ceramides; SM, sphingomyelinl; TAGs, triacylglycerides; HAfp, influenza hemagglutinin fusion peptide; Lck-cSH2, C-terminal Src Homology domain of Lymphocyte-specific protein-tyrosine kinase; DPC,

dodecylphosphocholine; DHPC, dihexanoylphosphatidylcholine; DAGK, diacylglycerol kinase; MSPs, membrane scaffold proteins; MAS, magic angle spinning; RDCs, residual dipolar couplings; PIP3-DPPC, Phosphatidylinositol-3,4,5-triphosphate C-16; RMSD, root-mean square deviations; SVD, singular value decomposition; PVDF, polyvinyldene difluoride; MALDI, matrix-assisted laser desorption ionization; LED-BPP, Bipolar Pulse Pairs; E-Bicelles, egg yolk derived bicelles; MB-Bicelles, mouse cerebrum derived bicelles; PB-Bicelles, procine brain derived bicelles; CL, cardiolipin; U, unidentified lipids; PIP, phosphatidylinositol phosphate; PIP2, phosphatidylinositol 4,5-bisphosphate; PIP3, Phosphatidylinositol 3,4,5-trisphosphate; CSP, chemical shift perturbations; DOSY, Diffusion ordered spectroscopy; SMA, styrene maleic acid.

REFERENCES

(1) Yang, S.-T., Kiessling, V., Simmons, J. A., White, J. M., and Tamm, L. K. (2015) HIV gp41-mediated membrane fusion occurs at edges of cholesterol-rich lipid domains. *Nat. Chem. Biol. 11*, 1–10.

(2) Kim, S. S., Upshur, M. A., Saotome, K., Sahu, I. D., McCarrick, R. M., Feix, J. B., Lorigan, G. A., and Howard, K. P. (2015) Cholesterol dependent conformational exchange of the C-terminal domain of the influenza A M2 protein. *Biochemistry 54*, 7157–7167.

(3) Miller, M. E., Adhikary, S., Kolokoltsov, A. A., and Davey, R. A. (2012) Ebolavirus Requires Acid Sphingomyelinase Activity and Plasma Membrane Sphingomyelin for Infection. *J. Virol. 86*, 7473–7483.

(4) Brown, D. A., and London, E. (2000) Structure and function of sphingolipid- and cholesterol-rich membrane rafts. *J. Biol. Chem. 275*, 17221–17224.

(5) Wang, S., Lee, S.-J., Heyman, S., Enkvetchakul, D., and Nichols, C. G. (2012) Structural rearrangements underlying ligand-gating in Kir channels. *Nat. Commun. 3*, ncomms1625.

(6) Lee, S.-J., Wang, S., Borschel, W., Heyman, S., Gyore, J., and Nichols, C. G. (2013) Secondary anionic phospholipid binding site and gating mechanism in Kir2.1 inward rectifier

channels. *Nat. Commun. 4*, ncomms3786.

(7) Dürr, U. H. N., Gildenberg, M., and Ramamoorthy, A. (2012) The magic of bicelles lights up membrane protein structure. *Chem. Rev. 112*, 6054–6074.

(8) Ujwal, R., and Bowie, J. U. (2011) Crystallizing membrane proteins using lipidic bicelles. *Methods 55*, 337–341.

(9) Ye, W., Lind, J., Eriksson, J., and Mäler, L. (2014) Characterization of the morphology of fast-tumbling bicelles with varying composition. *Langmuir 30*, 5488–5496.

(10) Yang, Z., Wang, C., Zhou, Q., An, J., Hildebrandt, E., Aleksandrov, L. A., Kappes, J. C., DeLucas, L. J., Riordan, J. R., Urbatsch, I. L., Hunt, J. F., and Brouillette, C. G. (2014) Membrane protein stability can be compromised by detergent interactions with the extramembranous soluble domains. *Protein Sci. 23*, 769–789.

(11) Jensen, M., and Mouritsen, O. G. (2004) Lipids do influence protein function - The hydrophobic matching hypothesis revisited. *Biochim. Biophys. Acta - Biomembr. 1666*, 205–226.

(12) Aimon, S., Callan-Jones, A., Berthaud, A., Pinot, M., Toombes, G. E. S., and Bassereau, P. (2014) Membrane Shape Modulates Transmembrane Protein Distribution. *Dev. Cell 28*, 212–218.

(13) Dill, K. A., and Flory, P. J. (1981) Molecular organization in micelles and vesicles. *Proc. Natl. Acad. Sci. U. S. A. 78*, 676–80.

(14) Fong, T. M., and McNamee, M. G. (1986) Correlation between Acetylcholine Receptor Function and Structural Properties of Membranes. *Biochemistry 25*, 830–840.

(15) Lee, A. G. (2004) How lipids affect the activities of integral membrane proteins. *Biochim. Biophys. Acta - Biomembr. 1666*, 62–87.

(16) Seddon, J. M. (1996) Lyotropic Phase Behaviour of Biological Amphiphiles. *Berichte der Bunsengesellschaft für Phys. Chemie 100*, 380–393.

(17) Vinogradova, O., Badola, P., Czerski, L., Sonnichsen, F. D., and Sanders, C. R. (1997) Escherichia coli Diacylglycerol Kinase : A Case Study in the Application of Solution NMR Methods to an Integral Membrane Protein Periplasmic Space Bilayer Normal. *Biophys. J. 72*, 2688–2701.

(18) Schnell, J. R., and Chou, J. J. (2008) Structure and mechanism of the M2 proton channel of influenza A virus. *Nature 451*, 591–595.

(19) Cady, S. D., Schmidt-Rohr, K., Wang, J., Soto, C. S., DeGrado, W. F., and Hong, M. (2010) Structure of the amantadine binding site of influenza M2 proton channels in lipid bilayers. *Nature 463*, 689–692.

(20) Murray, D. T., Li, C., Gao, F. P., Qin, H., and Cross, T. A. (2014) Membrane protein structural validation by oriented sample solid-state NMR: Diacylglycerol kinase. *Biophys. J. 106*, 1559–1569.

(21) Hagn, F., Etzkorn, M., Raschle, T., and Wagner, G. (2013) Optimized phospholipid bilayer nanodiscs facilitate high-resolution structure determination of membrane proteins. *J. Am. Chem. Soc. 135*, 1919–1925.

(22) Nath, A., Atkins, W. M., and Sligar, S. G. (2007) Applications of Phospholipid Bilayer Nanodiscs in the Study of Membranes and Membrane Proteins. *Biochemistry 46*, 2059–2069.

(23) Denisov, I. G., and Sligar, S. G. (2017) Nanodiscs in Membrane Biochemistry and Biophysics. *Chem. Rev. 117*, 4669–4713.

(24) Orwick, M. C., Judge, P. J., Procek, J., Lindholm, L., Graziadei, A., Engel, A., Gröbner, G., and Watts, A. (2012) Detergent-free formation and physicochemical characterization of nanosized lipid-polymer complexes: Lipodisq. *Angew. Chemie - Int. Ed. 51*, 4653–4657.

(25) Frey, L., Lakomek, N.-A., Riek, R., and Bibow, S. (2016) Micelles, Bicelles, and Nanodiscs: Comparing the Impact of Membrane Mimetics on Membrane Protein Backbone Dynamics. *Angew. Chemie Int. Ed.* 1–5.

(26) Serebryany, E., Zhu, G. A., and Yan, E. C. Y. (2012) Artificial membrane-like environments for in vitro studies of purified G-protein coupled receptors. *Biochim. Biophys. Acta - Biomembr. 1818*, 225–233.

(27) Brown, L. S., and Ladizhansky, V. (2015) Membrane proteins in their native habitat as seen by solid-state NMR spectroscopy. *Protein Sci. 24*, 1333–1346.

(28) Sackett, K., Nethercott, M. J., Zheng, Z., and Weliky, D. P. (2014) Solid-state NMR spectroscopy of the HIV gp41 membrane fusion protein supports intermolecular antiparallel ?? sheet fusion peptide structure in the final six-helix bundle state. *J. Mol. Biol. 426*, 1077–1094.

(29) Majumder, S., Xue, J., DeMott, C. M., Reverdatto, S., Burz, D. S., and Shekhtman, A. (2015) Probing Protein Quinary Interactions by in-cell NMR. *Biochemistry 54*, 2727-2738.

(30) Sakakibara, D., Sasaki, A., Ikeya, T., Hamatsu, J., Hanashima, T., Mishima, M., Yoshimasu, M., Hayashi, N., Mikawa, T., Wälchli, M., Smith, B. O., Shirakawa, M., Güntert, P., and Ito, Y. (2009) Protein structure determination in living cells by in-cell NMR spectroscopy. *Nature 458*,

102–105.

(31) Luchinat, E., and Banci, L. (2016) A Unique Tool for Cellular Structural Biology: In-cell NMR. *J. Biol. Chem. 291*, 3776 –3784.

(32) Gustavsson, M., Traaseth, N. J., and Veglia, G. (2012) Probing ground and excited states of phospholamban in model and native lipid membranes by magic angle spinning NMR spectroscopy. *Biochim. Biophys. Acta - Biomembr. 1818*, 146–153.

(33) Wu, H., Su, K., Guan, X., Sublette, M. E., and Stark, R. E. (2010) Assessing the size, stability, and utility of isotropically tumbling bicelle systems for structural biology. *Biochim. Biophys. Acta - Biomembr. 1798*, 482–488.

(34) Yamamoto, K., Pearcy, P., Lee, D.-K., Yu, C., Im, S.-C., Waskell, L., and Ramamoorthy, A. (2015) Temperature-resistant bicelles for structural studies by solid-state NMR spectroscopy. *Langmuir 31*, 1496–504.

(35) Chou, J. J., Kaufman, J. D., Stahl, S. J., Wingfield, P. T., and Bax, A. (2002) Micelle-induced curvature in a water-insoluble HIV-1 Env peptide revealed by NMR dipolar coupling measurement in stretched polyacrylamide gel. *J. Am. Chem. Soc. 124*, 2450–2451.

(36) Liebau, J., Pettersson, P., Zuber, P., Ariöz, C., and Mäler, L. (2016) Fast-tumbling bicelles constructed from native Escherichia coli lipids. *Biochim. Biophys. Acta - Biomembr. 1858*, 2097–2105.

(37) Marty, M. T., Wilcox, K. C., Klein, W. L., and Sligar, S. G. (2013) Nanodisc-solubilized membrane protein library reflects the membrane proteome. *Anal. Bioanal. Chem. 405*, 4009–4016.

(38) Smrt, S. T., Draney, A. W., and Lorieau, J. L. (2015) The influenza hemagglutinin fusion domain is an amphipathic helical hairpin that functions by inducing membrane curvature. *J. Biol. Chem. 290*, 228–38.

(39) Thiagarajan-Rosenkranz, P., Draney, A. W. A. W., Smrt, S. T. S. T., and Lorieau, J. L. (2015) A Positively Charged Liquid Crystalline Medium for Measuring Residual Dipolar Couplings in Membrane Proteins by NMR. *J. Am. Chem. Soc. 137*, 11932–11934.

(40) Sheng, R., Jung, D., Silkov, A., Singaram, I., Kim, H., Wang, Z., Xin, Y., Kim, E., Park, M., Thiagarajan-Rosenkranz, P., Smrt, S., Honig, B., Baek, K., Ryu, S., Lorieau, J., Kim, Y., and Cho, W. (2016) Lipids regulate Lck activity through their interactions with the Lck SH2 domain *. J. Biol. Chem. 291*, 17639–17650.

(41) Mills, R. (1973) Self-diffusion in normal and heavy water in the range 1-45.deg. *J. Phys. Chem. 77*, 685–688.

(42) Schweimer, K., Kiessling, A., Bauer, F., Hör, S., Hoffmann, S., Rösch, P., and Sticht, H. (2003) Letter to the Editor: Sequence-specific 1H, 13C and 15N resonance assignments of the SH3-SH2 domain pair fromthe human tyrosine kinase Lck. *J. Biomol. NMR 27*, 405–406.

(43) Kay, L. E., Keifer, P., and Saarinen, T. (1992) Pure absorption gradient enhanced heteronuclear single quantum correlation spectroscopy with improved sensitivity. *J. Am. Chem. Soc. 114*, 10663–10665.

(44) Wishart, D. S., Sykes, B. D., and Richards, F. M. (1991) Relationship between nuclear magnetic resonance chemical shift and protein secondary structure. *J. Mol. Biol. 222*, 311–333.

(45) Williamson, M. P. (2013) Using chemical shift perturbation to characterise ligand binding.

Prog. Nucl. Magn. Reson. Spectrosc. 73, 1–16.

(46) Ottiger, M., Delaglio, F., and Bax, A. (1998) Measurement of J and dipolar couplings from simplified two-dimensional NMR spectra. *J. Magn. Reson. 131*, 373–378.

(47) Delaglio, F., Grzesiek, S., Vuister, G. W., Zhu, G., Pfeifer, J., and Bax, A. (1995) NMRPipe: a multidimensional spectral processing system based on UNIX pipes. *J. Biomol. NMR 6*, 277–293.

(48) Goddard, T., and Kneller, D. Sparky 3. University of California, San Francisco.

(49) Lorieau, J. L., Louis, J. M., and Bax, A. (2010) The complete influenza hemagglutinin fusion domain adopts a tight helical hairpin arrangement at the lipid:water interface. *Proc. Natl. Acad. Sci. U. S. A. 107*, 11341–11346.

(50) Losonczi, J. A., Andrec, M., Fischer, M. W. F., and Prestegard, J. H. (1999) Order matrix analysis of residual dipolar couplings using singular value decomposition. *J. Magn. Reson. 138*, 334–342.

(51) Ottiger, M., and Bax, A. (1999) Bicelle-based liquid crystals for NMR-measurement of dipolar couplings at acidic and basic pH values. *J. Biomol. NMR 13*, 187–191.

(52) Cavanagh, J., Fairbrother, W., Palmer III, A., Rance, M., and Skelton, N. (2007) Protein NMR spectroscopy. Principles and Practice. *Elselvier Acad. Press*.

(53) London, E., and Feigenson, G. W. (1979) Phosphorus NMR analysis of phospholipids in detergents. *J. Lipid Res. 20*, 408–412.

(54) Sotirhos, N., Herslöf, B., and Kenne, L. (1986) Quantitative analysis of phospholipids by

31P-NMR. *J. Lipid Res. 27*, 386–392.

(55) Mannina, L., Cristinzio, M., Sobolev, A. P., Ragni, P., and Segre, A. (2004) High-Field Nuclear Magnetic Resonance (NMR) Study of Truffles (Tuber aestivum vittadini). *J. Agric. Food Chem. 52*, 7988–7996.

(56) Dannenberger, D., Süss, R., Teuber, K., Fuchs, B., Nuernberg, K., and Schiller, J. (2010) The intact muscle lipid composition of bulls: an investigation by MALDI-TOF MS and 31P NMR. *Chem. Phys. Lipids 163*, 157–64.

(57) Sommerer, D., Süß, R., Hammerschmidt, S., Wirtz, H., Arnold, K., and Schiller, J. (2004) Analysis of the phospholipid composition of bronchoalveolar lavage (BAL) fluid from man and minipig by MALDI-TOF mass spectrometry in combination with TLC. *J. Pharm. Biomed. Anal. 35*, 199–206.

(58) Teuber, K., Schiller, J., Fuchs, B., Karas, M., and Jaskolla, T. W. (2010) Significant sensitivity improvements by matrix optimization: A MALDI-TOF mass spectrometric study of lipids from hen egg yolk. *Chem. Phys. Lipids 163*, 552–560.

(59) Fuchs, B., Schiller, J., Süß, R., Schürenberg, M., and Suckau, D. (2007) A direct and simple method of coupling matrix-assisted laser desorption and ionization time-of-flight mass spectrometry (MALDI-TOF MS) to thin-layer chromatography (TLC) for the analysis of phospholipids from egg yolk. *Anal. Bioanal. Chem. 389*, 827–834.

(60) Metz, K. R., and Dunphy, L. K. (1996) Absolute quantitation of tissue phospholipids using 31P NMR spectroscopy. *J. Lipid Res. 37*, 2251–65.

(61) Tkac, I., Henry, P. G., Andersen, P., Keene, C. D., Low, W. C., and Gruetter, R. (2004)

Highly resolved in vivo 1H NMR spectroscopy of the mouse brain at 9.4 T. *Magn. Reson. Med.* *52*, 478–484.

(62) Macala, L. J., Yu, R. K., and Ando, S. (1983) Analysis of brain lipids by high performance thin-layer chromatography and densitometry. *J. Lipid Res.* *24*, 1243–1250.

(63) Essén-Gustavsson, B., and Tesch, P. A. (1990) Glycogen and triglyceride utilization in relation to muscle metabolic characteristics in men performing heavy-resistance exercise. *Eur. J. Appl. Physiol. Occup. Physiol.* *61*, 5–10.

(64) Tjandra, N., and Bax, A. (1997) Direct Measurement of Distances and Angles in Biomolecules by NMR in a Dilute Liquid Crystalline Medium. *Science (80-.).* *278*, 1111–1114.

(65) Folch, J., Lees, M., and Stanley, G. H. S. (1957) A Simple Method for the Isolation and Purification of Total Lipides From Animal Tissues. *J. Biol. Chem.* *226*, 497–509.

(66) Kovacs-Nolan, J., and Mine, Y. (2004) Avian egg antibodies: basic and potential applications. *Avian Poult. Biol. Rev.* *15*, 25–46.

(67) Kuksis, A. (1992) Yolk lipids. *Biochim. Biophys. Acta* *1124*, 205–222.

(68) Müller, M., Schiller, J., Petković, M., Oehrl, W., Heinze, R., Wetzker, R., Arnold, K., and Arnhold, J. (2001) Limits for the detection of (poly-)phosphoinositides by matrix-assisted laser desorption and ionization time-of-flight mass spectrometry (MALDI-TOF MS). *Chem. Phys. Lipids* *110*, 151–164.

(69) Anderson, K. E., Kielkowska, A., Durrant, T. N., Juvin, V., Clark, J., Stephens, L. R., and Hawkins, P. T. (2013) Lysophosphatidylinositol-Acyltransferase-1 (LPIAT1) Is Required to

Maintain Physiological Levels of PtdIns and PtdInsP2 in the Mouse. *PLoS One 8*, e58425.

(70) Vanhaesebroeck, B., Leevers, S. J., Timms, J., Katso, R., Driscoll, P. C., Woscholski, R., Parker, P. J., and Michael, D. (2001) Synthesis and Function of 3-Phosphorylated Inositol Lipids. *Annu. Rev. Biochem. 70*, 535–602.

(71) Heiny, A. T., Miotto, O., Srinivasan, K. N., Khan, A. M., Zhang, G. L., Brusic, V., Tan, T. W., and August, J. T. (2007) Evolutionarily conserved protein sequences of influenza a viruses, avian and human, as vaccine targets. *PLoS One 2*, e1190.

(72) Lorieau, J. L. J., Louis, J. M. J., and Bax, A. (2011) Helical Hairpin Structure of Influenza Hemagglutinin Fusion Peptide Stabilized by Charge− Dipole Interactions between the N-Terminal Amino Group and the Second. *J. Am. Chem. Soc. 133*, 2824–2827.

(73) Robertson, J. S., Cook, P., Attwell, A. M., and Williams, S. P. (1995) Replicative advantage in tissue culture of egg-adapted influenza virus over tissue-culture derived virus: implications for vaccine manufacture. *Vaccine 13*, 1583–1588.

(74) Lindberg, M., Biverståhl, H., Gräslund, A., and Mäler, L. (2003) Structure and positioning comparison of two variants of penetratin in two different membrane mimicking systems by NMR. *Eur. J. Biochem. 270*, 3055–3063.

(75) Lau, T. L., Partridge, A. W., Ginsberg, M. H., and Ulmer, T. S. (2008) Structure of the integrin _β3 transmembrane segment in phospholipid bicelles and detergent micelles. *Biochemistry 47*, 4008–4016.

(76) Vinogradova, O., Sönnichsen, F., and Sanders, C. R. (1998) On choosing a detergent for solution NMR studies of membrane proteins. *J. Biomol. NMR 11*, 381–386.

(77) Warschawski, D. E., Arnold, A. A., Beaugrand, M., Gravel, A., Chartrand, É., and Marcotte, I. (2011) Choosing membrane mimetics for NMR structural studies of transmembrane proteins. *Biochim. Biophys. Acta - Biomembr. 1808*, 1957–1974.

(78) Poget, S. F., and Girvin, M. E. (2007) Solution NMR of membrane proteins in bilayer mimics: Small is beautiful, but sometimes bigger is better. *Biochim. Biophys. Acta - Biomembr. 1768*, 3098–3106.

(79) Lorieau, J. L., Maltsev, A. S., Louis, J. M., and Bax, A. (2013) Modulating alignment of membrane proteins in liquid-crystalline and oriented gel media by changing the size and charge of phospholipid bicelles. *J. Biomol. NMR 55*, 369–377.

(80) Mineev, K. S., Nadezhdin, K. D., Goncharuk, S. A., and Arseniev, A. S. (2016) Characterization of Small Isotropic Bicelles with Various Compositions. *Langmuir 32*, 6624–6637.

(81) Beaugrand, M., Arnold, A. a., Hénin, J., Warschawski, D. E., Williamson, P. T. F., and Marcotte, I. (2014) Lipid concentration and molar ratio boundaries for the use of isotropic bicelles. *Langmuir 30*, 6162–6170.

(82) Lorieau, J. L., Louis, J. M., and Bax, A. (2011) Whole-body rocking motion of a fusion peptide in lipid bilayers from size-dispersed 15N NMR relaxation. *J. Am. Chem. Soc. 133*, 14184–14187.

(83) Chou, J. J., Baber, J. L., and Bax, A. (2004) Characterization of phospholipid mixed micelles by translational diffusion. *J. Biomol. NMR 29*, 299–308.

(84) Eck, M. J., Atwell, S. K., Shoelson, S. E., and Harrison, S. C. (1994) Structure of the

regulatory domains of the Src-family tyrosine kinase Lck. *Nature 368*, 764–769.

(85) Park, M.-J. J., Sheng, R., Silkov, A., Jung, D.-J. J., Wang, Z.-G. G., Xin, Y., Kim, H., Thiagarajan-Rosenkranz, P., Song, S., Yoon, Y., Nam, W., Kim, I., Kim, E., Lee, D.-G. G., Chen, Y., Singaram, I., Wang, L., Jang, M. H. H., Hwang, C.-S. S., Honig, B., Ryu, S., Lorieau, J., Kim, Y.-M. M., and Cho, W. (2016) SH2 Domains Serve as Lipid-Binding Modules for pTyr-Signaling Proteins. *Mol. Cell 62*, 7–20.

(86) Wharton, S. S. a, Martin, S. R., Ruigrok, R. W., Skehel, J. J., and Wiley, D. C. (1988) Membrane fusion by peptide analogues of influenza virus haemagglutinin. *J. Gen. Virol. 69*, 1847–1857.

(87) Domanska, M. K., Dunning, R. A., Dryden, K. A., Zawada, K. E., Yeager, M., and Kasson, P. M. (2015) Hemagglutinin Spatial Distribution Shifts in Response to Cholesterol in the Influenza Viral Envelope. *Biophys. J. 109*, 1917–1924.

(88) Schnaitman, C. a. (1970) Protein Composition of the Cell Wall and Cytoplasmic Membrane of Escherichia coli. *J. Bacteriol. 104*, 890–901.

(89) Allen, R. D., Schroeder, C. C., and Fok, A. K. (1989) An investigation of mitochondrial inner membranes by rapid-freeze deep-etch techniques. *J. Cell Biol. 108*, 2233–2240.

(90) Fujiki, Y., Hubbard, A. L., Fowler, S., and Lazarow, P. B. (1982) Isolation of Intracellular Membranes by Means of Sodium-Carbonate Treatment - Application to Endoplasmic-Reticulum. *J. Cell Biol. 93*, 97–102.

(91) Blobel, G., and Van R. Potter. (1966) Nuclei from Rat Liver: Isolation Method Tht Combines Purity with High Yield. *Science (80-.). 154*, 1662–1665.

TOC